Eur. Phys. J. B **48**, 509–517 (2005)
DOI: 10.1140/epjb/e2006-00004-6

THE EUROPEAN PHYSICAL JOURNAL B

Thermal conductivity associated with a bead-bead contact decorated by a liquid bridge

An experimental study based on the response of a chain subjected to thermal cycles

J.-C. Géminard[a], D. Bouraya, and H. Gayvallet

Laboratoire de Physique de l'ENS de Lyon, 46 Allée d'Italie, 69364 Lyon Cedex 07, France

Received 24 March 2005 / Received in final form 2 June 2005
Published online 19 January 2006 –

Abstract. We report an experimental study of the heat transport along a chain of macroscopic beads: at one end, one bead is periodically heated and we record the resulting temperature variations of another bead as a function of position and time. The experimental results show that the chain behaves like a high-order low-pass filter. The measurement of the associated cut-off frequency makes it possible to determine accurately the resistance of the bead-bead contact: we make use of the experimental setup for studying the effects of liquid bridges decorating the bead-bead contacts, which provides important clues for understanding the thermal properties of partially wet granular matter.

PACS. 66.70.+f Nonelectronic thermal conduction and heat-pulse propagation in solids; thermal waves – 81.05.Rm Porous materials; granular materials – 91.60.Ki Thermal properties

1 Introduction

The transport of electricity, sound or heat in a dense assembly of solid particles poses interesting and puzzling questions. Even if granular materials are widely used in industry, one is still far from understanding entirely how the transport coefficients relate to the physics of the contacts between the particles and the geometry of the contact network (*texture*). For instance, for over a century [1,2], electrical transport in metallic powders has generated interest. These systems exhibit fascinating properties, such as highly non-linear and hysteretic electrical conductivities as well as extreme sensitivity to electromagnetic waves [3]. The propagation of soundwaves in granular materials also exhibits very interesting features; non-linearities such as a slight dependence of the transmission amplitude on the frequency of the source at low vibration amplitude and an extreme sensitivity to the position of each grain [4]. The propagation of soundwaves is so sensitive to the texture that it is likely to be altered by the vibration itself or by small changes in the temperature. However, the propagation of non-linear waves in a one-dimensional chain of beads under static stress has been experimentally proven to follow the prediction of Hertz theory as long as plastic deformations of the grains at the contacts are not involved [5].

In the same way, the transport of heat in granular materials poses puzzling questions which need to be answered as thermal properties of granular matter are of great practical importance. Indeed, the most common materials used to insure thermal as well as acoustic insulation in buildings consist of assemblies of solid particles or fibers. For instance, glasswools are efficient thermal insulators that also present the advantage of being low-cost, imputrescible and fire resistant as they are produced mainly from recycled glass and sand [6]. Moreover, because of their ductility, they can absorb any unevenness of the substrate. Another important application worthy of mention here is the use of granular materials as buffers in nuclear-waste deposits [7]. Experimental and theoretical studies of the heat transport in granular materials have already been reported [2,8–10]. They pointed out the crucial role played by the physics of the contacts between the grains. Accordingly, humidity has been experimentally proven to increase significantly the thermal conductivity as water tends to decorate the contact points [11].

Whereas this latter study considered the thermal properties of the bulk granular material, involving thus the texture of the material, there does not exist, to our knowledge, any experimental study dedicated to the thermal properties of the decorated contacts alone. In the present article, we report an experimental study of the thermal conductivity of a one-dimensional chain of beads. This is in the same spirit as preceding studies of electric conductivity [3] and sound propagation [5] that made it possible

[a] e-mail: jean-christophe.geminard@ens-lyon.fr

to analyze the physics of the contacts in the absence of texture effects. The response of the system to temperature cycles shows that a periodic medium can be an efficient thermal-insulator in the sense that, for instance, the chain is very efficient in filtering temperature changes as it acts as a high-order low-pass filter. We determine the corresponding cut-off frequency in order to obtain reliable measurements of the thermal resistance associated with the bead-bead contact. We make use of the experimental setup for studying the effects of liquid bridges decorating the bead-bead contacts.

The content of the manuscript is organized as follows: in Section 2, we introduce the principle of the experiment and describe the experimental setup and procedure. In Section 3, we report our experimental results obtained in the cases of dry or wet contacts and compare with theoretical predictions. Finally, we conclude in Section 4.

2 Experimental setup and procedure

The experiment consists of heating periodically one end of a linear chain of beads and recording the resulting temperature of the nth bead as a function of time t. In the next Section 2.1, we describe the experimental setup whereas the Section 2.2 is dedicated to the procedure used to analyze the thermal response of the system to the heat injection (Fig. 1).

2.1 Experimental setup

The chain consists of 10 centimetre-sized ball-bearing steel-beads (AISI 304, diameter $d = 1$ cm, from Marteau & Lemarié) aligned with the help of three PTFE plates [see the chain cross-section in the inset (Fig. 1)] that insure a relatively small thermal contact with the remaining part of the experimental setup which consists of a stainless steel frame. The contact between the beads is insured by pushing (static axial force F) the chain at one end against a fixed steel cylinder located at the other end. A force sensor (Entran, ELA-B2E-10KN) is used to measure F to within 10 N ($F < 10$ kN).

In order to inject heat at one end of the chain, the first bead is equipped with a small heating wire (Constantan, diameter 100 μm, typical resistance $r \simeq 1\ \Omega$) placed at its center. We impose the periodic voltage $U(t) = U_0\big(1+\sin 2\pi\nu t\big)$ from a home-made linear power-amplifier driven by a function generator (Stanford Research Systems, DS345). A first multimeter (Keithley 2001) is used to measure the voltage difference $U(t)$ across the heat source (Fig. 2). In our experimental conditions, the frequency ν ranges from 1/3600 to 1/30 Hz whereas the maximum voltage $2U_0$ is about 3 V. The power $P(t)$ injected in the first bead is thus written:

$$P(t) = P_0\left[\frac{3}{4} + \sin 2\pi\nu t + \frac{1}{4}\sin\left(4\pi\nu t + \frac{3\pi}{2}\right)\right] \qquad (1)$$

where $P_0 = 2U_0^2/r$ (we neglect here the variation of r with the temperature). We point out that the bead is continuously heated with a mean power $\frac{3}{4}P_0$ and that the variation with time of the heating power $P(t)$ contains two harmonics. We shall make use of this latter property for studying simultaneously the response of the system at the three frequencies 0, ν and 2ν.

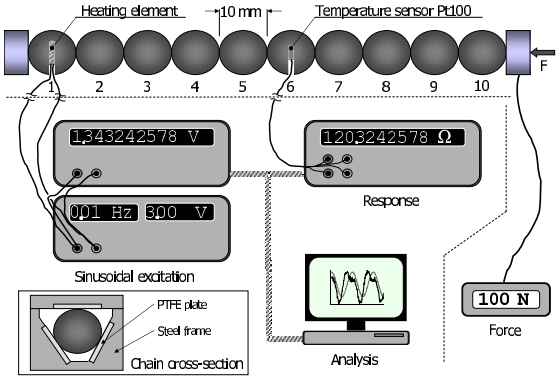

Fig. 1. Sketch of the experimental principle. The chain consists of 10 centimetre-sized steel-beads aligned with the help of three PTFE plates (inset). In order to insure the contact between the beads, a static force F is applied at one end (bead 10). The first bead (bead 1) is heated by means of a small resistive wire located at its center: the heating voltage is measured by means of a first multimeter. In order to obtain the local temperature of the chain, the bead n ($n = 6$ in the sketched situation) is equipped with a Pt-sensor whose resistance is measured with the help of a second multimeter. In addition, the temperature of the surrounding air, between beads 7 and 8, is measured by means of a second Pt-sensor (not sketched in this figure).

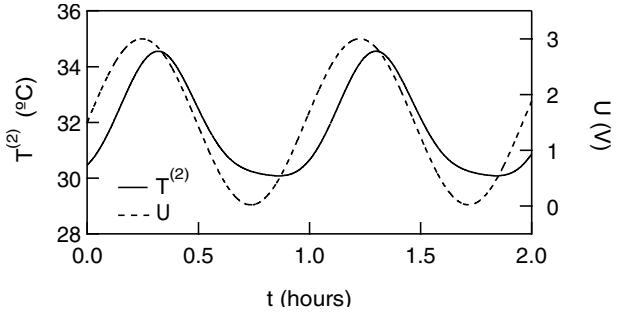

Fig. 2. Experimental $T^{(2)}$ and U vs. time t. We report, for $\nu = 1/3600$ Hz, the temperature $T^{(2)}$ of bead 2 and the voltage U as a function of time t during 2 hours in the permanent regime (the total duration of the experiment is 10 hours, corresponding to 10 periods of the excitation). The mean temperature is about 2.5 K above the temperature T_a of the surrounding air ($\delta T_0^{(2)} \simeq 2.5$ K). The amplitude of the temperature variations at ν is about 2.21 K whereas it is about 0.46 K at 2ν (dry contacts, $F = 100$ N).

The bead n (the index n refers to the position of the bead in the chain) is equipped with a temperature sensor (Pt100, from Heraeus) located at its center. A second multimeter (Keithley 196), used in the 4-wire configuration, measures the resistance R_s of the sensor so that the local temperature of bead n, $T^{(n)}(t)$, is known to within about 10^{-3} K. As we do not regulate the overall temperature of the experimental setup, we measure, in addition, the outside air temperature, T_a, by means of a second temperature sensor (Pt100) located in air and connected to a third multimeter (Keithley 196).

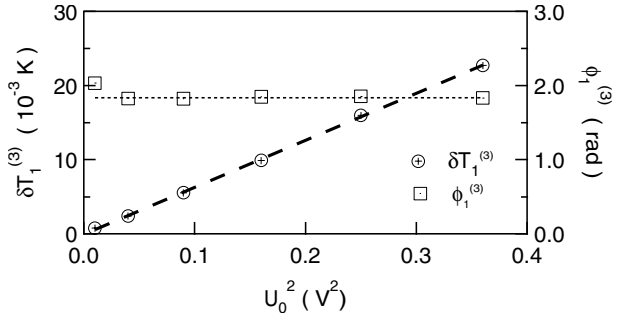

Fig. 3. Amplitude $\delta T_1^{(3)}$ and phase $\phi_1^{(3)}$ vs. U_0^2. As an example, we report the amplitude, $\delta T_1^{(3)}$, and phase, $\phi_1^{(3)}$, measured for bead 3 as a function of the square heating-voltage U_0^2. The amplitude of the harmonics $\delta T_{1(,2)}^{(n)}$ is proportional to U_0^2 and the phase $\Phi_{1(,2)}^{(n)}$ does not depend on U_0, which proves that the response of the system is linear.

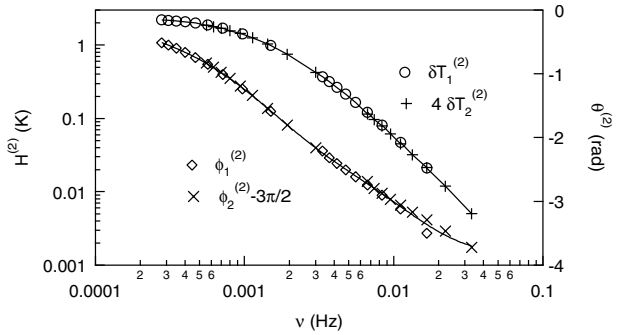

Fig. 4. Experimental $H^{(2)}$ and $\theta^{(2)}$ vs. frequency ν. As an example, we report the amplitude, $H^{(2)}$, and the phase, $\theta^{(2)}$, as a function of the frequency ν. The data evaluated from the first or the second harmonics are marked with different symbols. We observe that the responses estimated from the first and second harmonics respectively superpose down to temperature variations with an amplitude of about 10^{-3} K (the lines are only a guide for the eye).

The function generator and the three multimeters are connected to a computer through a IEEE interface. For a given set of experimental conditions (position n of the sensing bead, applied force F, dry or wet contacts), a simple C-routine automates the experiment: for a chosen set of heating powers P_0 and frequencies ν, the voltage $U(t)$ and the temperature $T^{(n)}(t)$ are measured (sampling frequency 1 Hz) and saved to the hard-drive (Fig. 2). Analysis of the data is performed afterwards (Igor Pro 4, WaveMetrics, Inc.).

2.2 Transfer function

From equation (1), if the system has a linear response, we expect the temperature $T^{(n)}(t)$ to exhibit the same spectral components as $P(t)$, that is to say, harmonics at frequencies 0, ν and 2ν. From the raw data (Fig. 2), we extract five relevant quantities; the amplitudes, $\delta T_1^{(n)}$ and $\delta T_2^{(n)}$, the phases, $\phi_1^{(n)}$ and $\phi_2^{(n)}$, of the two harmonics at the frequencies ν and 2ν and the mean temperature difference $\delta T_0^{(n)}$ between the bead n and the outside atmosphere (0 frequency). To do so, we interpolate the experimental temperature-difference $\Delta T^{(n)}(t) \equiv T^{(n)}(t) - T_a$ with

$$\Delta T^{(n)}(t) = \delta T_0^{(n)} + \delta T_1^{(n)} \sin\left(2\pi\nu t + \phi_1^{(n)}\right) + \delta T_2^{(n)} \sin\left(4\pi\nu t + \phi_2^{(n)}\right). \quad (2)$$

The origin of time t in equation (2) is accurately obtained by interpolating $U(t)$ with a sine-function and by choosing the origin such that $U(0) = U_0$ and $\frac{dU}{dt}(0) > 0$.

We first check that the response of the system is linear: the amplitude of each of the harmonics, $\delta T_{1(,2)}^{(n)}$, scales as U_0^2 (thus, is proportional to the heating power) whereas the corresponding phase, $\phi_{1(,2)}^{(n)}$, does not depend on U_0 (Fig. 3).

Thus, from the quantities $\delta T_0^{(n)}$, $\delta T_1^{(n)}$, $\delta T_2^{(n)}$, $\phi_1^{(n)}$ and $\phi_2^{(n)}$, we can determine experimentally the power-to-(temperature of the bead n) transfer-function, $\underline{H}^{(n)}(\nu) \equiv H^{(n)} e^{j\theta^{(n)}}$, as follows: a first set of data points is obtained from the first harmonics at the frequency ν. From the first harmonics, we get $H^{(n)} = \delta T_1^{(n)}$ and $\theta^{(n)} = \phi_1^{(n)}$. In equation (1), we notice that the power injected in the first harmonic at ν is 4 times larger than that injected in the second harmonic at 2ν, and that there is a phase-shift of $\frac{3\pi}{2}$ between them. Thus, from the same experiment, the second harmonic provides another set of data points with $H^{(n)} = 4\delta T_2^{(n)}$ and $\theta^{(n)} = \phi_2^{(n)} - \frac{3\pi}{2}$ at the frequency 2ν. Note that, by construction, $H^{(n)}$ has the dimension of temperature and is proportional to P_0. Strictly speaking, we should divide $H^{(n)}$ by P_0 to get the power-to-(temperature of the bead n) transfer-function, but, as we will not change P_0 in what follows, we will report $H^{(n)}$ as the temperature defined above. In Figure 4, we report a typical experimental result for $\underline{H}^{(2)}(\nu)$. We observe that the data evaluated from the first and second harmonics superpose down to temperature variations with an amplitude of about 10^{-3} K.

We shall explain in the section devoted to the experimental results (Sect. 3) how the response of the chain can be extracted from these data, provided we are able to model the response of the experimental setup.

2.3 Experimental procedure

The experimental procedure is as follows: for the chosen experimental conditions (applied force F, dry or wet contacts), in order to obtain the response of the system, we first place the bead containing the temperature sensor at a chosen position n. For a series of excitation frequencies ν, we record the temperature variation $T^{(n)}$ as a function of time t in the permanent regime. The response at a different position n is obtained after opening the experimental setup and changing the position of the sensing bead. The experimental procedure makes it possible to determine $\underline{H}^{(n)}(\nu)$ for $n \in [2, 7]$ in the frequency

range $1/\nu \in [30, 3600]$ s. Measurements at frequencies smaller than 1/3600 Hz are, in principle, possible but note that we record the temperature variations for 10 periods, which then would lead to an experimental time larger than 10 hours. For frequencies larger than 1/30 Hz, the temperature variations become small (the amplitude is typically less than 10^{-3} K) and the response of the system is determined with poor accuracy. We always make sure that the measurements are reliable by checking that the phase of the measured harmonics is locked (i.e. that the phase is not arbitrary with respect to that of the heating voltage) and exclude the data points that do not satisfy this condition.

3 Experimental results

In the following section, we make use of the experimental setup for studying the thermal properties of the chain under different experimental conditions. In the next Section 3.1, we consider the case of dry contacts in air: the analysis of the whole set of experimental data permits the modeling of the thermal response of the whole experimental setup. Then, Section 3.2 is dedicated to the study of wet contacts obtained by the addition of liquid droplets in the bead-bead contact-regions.

3.1 Dry contacts

3.1.1 First experimental observations

In Figures 5 and 6, we present the whole set of experimental data obtained for the chain of steel beads with dry contacts and $F = 100$ N (the static applied force is small and only insures that the beads are in contact). At first sight, the chain behaves like a low-pass filter whose order depends on the position n of the bead within the chain (the larger n is, the larger is the order of the filter). Nevertheless, we cannot immediately extract the characteristic frequency of the filter without exploring in detail the response of the experimental setup.

For instance, consider only the response of the system at zero frequency. Due to thermal losses, one would expect the mean temperature $\delta T_0^{(n)}$ (accordingly $H^{(n)}(0)$) to vanish (i.e. $T^{(n)}(t) \to T_a$) for $n \to \infty$. However, even if we observe that $H^{(n)}(0)$ decreases almost exponentially as n is increased, the mean temperature-difference $H^{(n)}(0)$ seems surprisingly to tend to a constant value for large n (typically larger than 7, Fig. 7). The decay of $H^{(n)}(0)$ to a finite temperature-difference is the most obvious experimental manifestation of the non-trivial response of the experimental setup. It turns out that, the response at zero frequency is not enough for us to measure the thermal losses to the outside atmosphere: the whole set of experimental data is necessary for obtaining a correct model of the experimental situation, which we discuss in the next section.

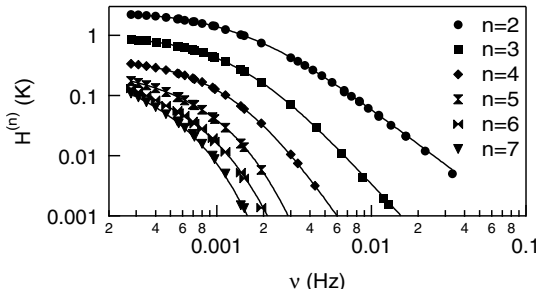

Fig. 5. Amplitude $H^{(n)}$ vs. frequency ν. The amplitude $H^{(n)}$ decreases faster with increasing frequency ν for larger n ($F = 100$ N, dry contacts, the lines are only guide for the eye).

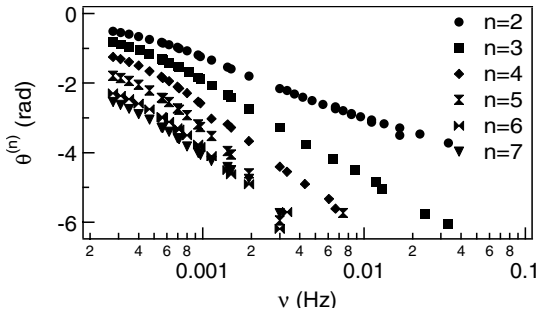

Fig. 6. Phase $\theta^{(n)}$ vs. frequency ν. The absolute phase-shift $\theta^{(n)}$ increases faster with increasing frequency ν for larger n ($F = 100$ N, dry contacts).

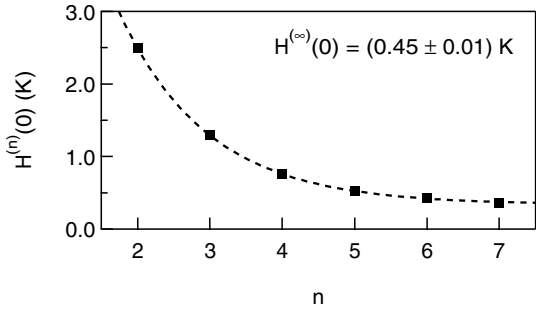

Fig. 7. Experimental $H^{(n)}(0)$ vs. bead position n. We observe that the temperature difference at zero frequency between the bead n and the atmosphere decreases almost exponentially as n increases and seems to tend to a constant value for large n.

3.1.2 Dynamical response

From the experimental data presented in Figure 5, we can extract the dependence of the amplitude $H^{(n)}$ on the position n at a given frequency ν (Fig. 8). We observe again that, even at non-zero frequency, the amplitude $H^{(n)}$ decreases almost exponentially as n is increased and seems to tend to a non-zero value for large n. Experimental data for $n > 7$ are not available and we cannot conclude rigorously that $H^{(n)}(\nu)$ vanishes for $n \to \infty$. However, $H^{(n)}(\nu)$ seems to reach a plateau value, $H^{(\infty)}(\nu)$, for n large compared to a typical number $1/k'(\nu)$. In order to define unambiguously $H^{(\infty)}(\nu)$ and $k'(\nu)$ from the experimental data, we interpolate the measurements for $n \in [2, 7]$ with:

$$H^{(n)}(\nu) = H^{(0)}(\nu) \exp\left[-k'(\nu)n\right] + H^{(\infty)}(\nu). \quad (3)$$

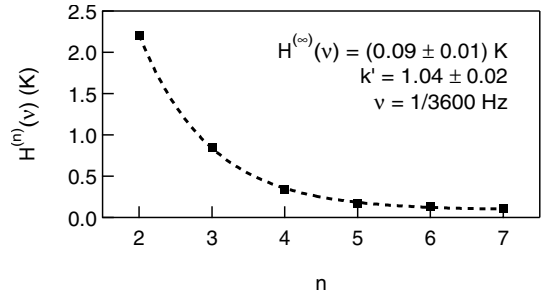

Fig. 8. Amplitude $H^{(n)}$ vs. bead position n. For a given frequency ν, the amplitude $H^{(n)}$ does not seem to vanish for large n. The result holds true in the frequency range explored experimentally and we find that the limit $H^{(\infty)}$ [defined by Eq.(3)] decreases when the frequency ν is increased (Fig. 9).

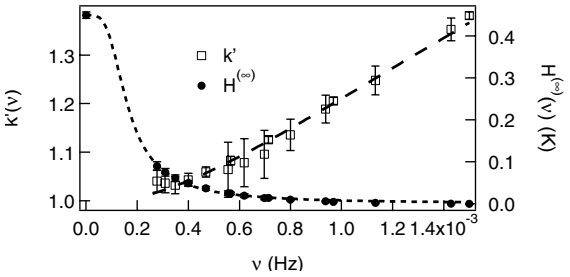

Fig. 9. Asymptotic amplitude $H^{(\infty)}$ and k' vs. ν. We observe experimentally that the asymptotic amplitude $H^{(\infty)}$ decreases, according to equation (4), when the frequency ν is increased. In addition, $k' = \Re(k)$ obeys equation (5), which makes it possible to characterize the thermal conduction along the chain.

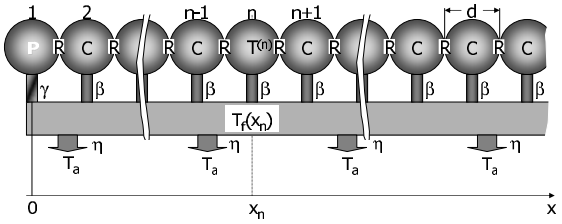

Fig. 10. Sketch of the experimental situation.

In Figure 9, we report the experimental values of $H^{(\infty)}(\nu)$ [Eq. (4)] and $k'(\nu) = \Re(k)$ [Eq. (5)] which can be accounted for by modeling the experimental situation as follows (Fig. 10): we consider the beads as heat capacitors (heat capacity C), each one connected to its two neighbors through thermal resistors (resistance R), and we assume that the thermal losses to the frame can be associated to the thermal resistance, β along the chain ($n \geq 2$) and γ at bead 1. A detailed description of the model is proposed in the appendix.

We observe a good agreement of the experimental data (Fig. 9) with

$$H^{(\infty)}(\nu) \sim \frac{1}{\sqrt{1+\left(\frac{2\pi\nu}{\omega_c}\right)^4}} \tag{4}$$

for $\omega_c = (0.8 \pm 0.01) \times 10^{-3}$ rad s^{-1} where $\omega_c^{-1} \equiv C\sqrt{\beta\gamma}$ from the model [see appendix, Eq. (18)]. In addition, we expect k' to be the real part of k, defined by

$$\cosh(k) = \left[1 + \frac{1}{\omega_0\tau_c}\right] + j\frac{2\pi\nu}{\omega_0}. \tag{5}$$

where $\omega_0^{-1} \equiv RC/2$ and $\tau_c \equiv \beta C$. From equation (5) and the experimental data, we get $\omega_0\tau_c = 1.87 \pm 0.03$ and $\omega_0 = (7.6 \pm 0.1) \times 10^{-3}$ rad s^{-1}. Note that the first quantity, $\omega_0\tau_c \equiv 2\beta/R$, is the ratio of the resistance β associated with the energy losses to the resistance R of the bead-bead contacts whereas $\omega_0 \equiv 2/(RC)$ characterizes the transport of heat along the chain alone.

3.1.3 Quantitative analysis

In this section, we shall compare the experimental value of the contact resistance, which we can extract from the experimental ω_0, with a theoretical model by Batchelor and O'Brien [2].

First, one can find in the literature the heat capacity $c_s = 0.5$ J g^{-1} K^{-1} and the density $\rho_s = 8$ g cm^{-3} of steel (AISI 304), which gives $C = 2.1$ J K^{-1} for $d = 1$ cm. Thus, from the experimental value of ω_0, one obtains the experimental value, $R_{exp} = (126 \pm 1)$ K W^{-1}, of the resistance of the bead-bead contact.

Second, we can consider theoretically the heat flux $\Psi \equiv (T^{(n)} - T^{(n+1)})/R$ from bead n to bead $(n+1)$. According to Hertz theory, due to the axial applied force F, the radius ρ of the contact region is given by [12]:

$$\rho = F^{1/3}\left[\frac{3(1-\sigma^2)d}{8E}\right]^{1/3} \tag{6}$$

where $E = 2 \times 10^{11}$ Pa is the Young modulus and $\sigma = 0.29$ the Poisson ratio of the material that the beads are made of. In our experimental conditions ($F = 100$ N), we find $\rho = 0.12$ mm. In addition, the heat conductivity of steel, $k_s = 16.2$ W m^{-1} K^{-1}, is large compared to the thermal conductivity of air, $k_a = 0.025$ W m^{-1} K^{-1}. Denoting $\zeta = k_s/k_a$ and $\xi = 2\zeta\rho/d$ (in our experimental conditions, $\zeta \simeq 650$ and, from the radius ρ of the contact region, $\xi \simeq 15.6$), we can write

$$\frac{2\Psi}{\pi k_a d(T^{(n)} - T^{(n+1)})} = \mathcal{H}_0(\zeta) + \mathcal{H}_c(\xi) + \Delta\mathcal{H}_m(\xi). \tag{7}$$

In equation (7), $\mathcal{H}_0(\zeta)$ stands for the dimensionless heat-flux across the air layer in the case of a point-like contact. Provided that $\zeta \gg 1$,

$$\mathcal{H}_0(\zeta) = 2\log_e\left(\frac{k_s}{k_a}\right) + A - 3.9 \tag{8}$$

where A is a constant of the order of unity which depends on the outer field conditions and is independent of ζ. The second contribution $\mathcal{H}_c(\xi)$ in equation (7) accounts for the dimensionless heat-flux across the contact circle of finite radius ρ. In the limit $\xi \gg 1$, $\mathcal{H}_c(\xi) \sim 2\xi/\pi$. We point out that, from [2], $\mathcal{H}_c(\xi)$ obeys this asymptotic behavior

typically for $\xi > 10$. Finally, the last contribution to the heat flux in equation (7), $\Delta\mathcal{H}_m(\xi)$ accounts for the difference between the real flux across the air layer and the flux expected in the case of a point-like contact. In the limit $\xi \gg 1$, $\Delta\mathcal{H}_m(\xi) \sim -2\log_e \xi$ but we note that this asymptotic behavior is expected for very large values of ξ. From the experimental value of ξ, we expect $\Delta\mathcal{H}_m(\xi) \simeq -0.5$ [2]. Finally, from equation (7), we obtain the theoretical value $R_{theo} = 2546/(18.5 + A)$ K W^{-1} which agrees quantitatively with the experimental value $R_{exp} \simeq 126$ K W^{-1} for $A \simeq 1.7$, which is of the order of unity. Thus, we conclude from the excellent agreement (in spite of the uncertainty in the value of A) between R_{exp} and R_{theo} that measurements of the frequency ω_0 provides reliable values of the contact resistance R.

In the next Section 3.2, we make use of the experimental setup for analyzing the effect of liquid bridges decorating the regions of contact between the beads.

3.2 Wet contacts

As already mentioned in the introduction, humidity has been experimentally proven to increase significantly the thermal conductivity of an assembly of glass beads as water decorates the contact points [11]. Our experimental setup is particularly suitable for studying the effects of liquid decorating the contact points. Indeed, a change of the physical conditions in the contact region is not expected to affect any of the model parameters (τ_c, τ_b, α as defined in the appendix) except the cut-off angular frequency ω_0, which relates to the resistance of the contact. Thus, one can save experimental time and study the evolution of ω_0 alone by analyzing the response of the system at a given position n only.

3.2.1 Experimental procedure

We shall report the evolution of the thermal resistance R of the bead-bead contact as a function of the size of the liquid bridges that decorate the contact regions. As an example, we choose to study the response of the system at bead 4. We know from the study of the dry system that the amplitude of the temperature variations is large enough for giving significant results and that the order of the 'filter' is also large enough to provide accurate measurements of the cut-off frequency ω_0. This choice is to a large extent arbitrary.

Non-volatile liquid bridges (identical along the chain) are created by placing a given amount of silicon oil (Rhodorsil, 47V5000) in each of the bead-bead contact-regions. We expect, from the large viscosity of the liquid ($\nu = 5000$ cP), the temperature gradient not to induce any significant convective flow and the transport of heat to be only due to diffusion. We image the system from the side (Fig. 11), which makes it possible to measure the diameter, Φ, of the liquid bridge (the variability along the chain remains less than 2%). We measure ϕ before and after measurement of the thermal response of the system in order to make sure that the bridges remain in equilibrium for the duration of the experiment.

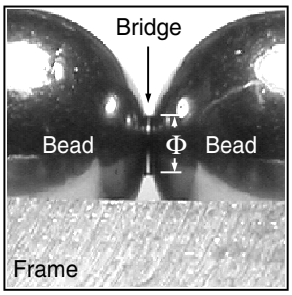

Fig. 11. Photograph of a liquid bridge. We measure the diameter Φ of the liquid bridge on photographs of the bead-bead contact-regions ($\Phi = 2.17$ mm, the lateral size of the photograph is 1 cm).

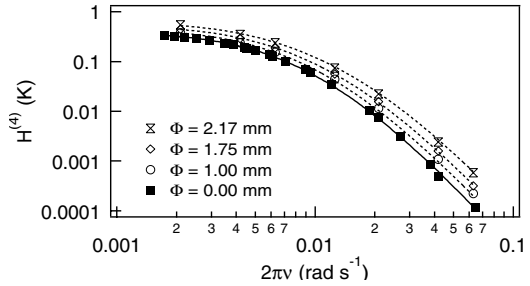

Fig. 12. Amplitude $H^{(4)}$ vs. $2\pi\nu$. The amplitude $H^{(4)}$ is affected by the presence of liquid bridges in the contact regions between the grains: we observe that, at a given frequency ν, $H^{(4)}$ increases with the diameter Φ of the bridges. The presence of the liquid leads to a decrease in the thermal resistance R of the contact. The experimental data (symbols) are successfully accounted for by the theoretical description of the system [lines, from equation (18) with different values of ω_0].

3.2.2 Results

We report in Figure 12, the amplitude $H^{(4)}$ as a function of the frequency ν for the dry system and three different diameters Φ. The experimental results exhibit an excellent agreement with the theoretical expression (18) in which we use the experimental parameters, $\tau_b = 318$ s, $\tau_c = 246$ s, $\alpha = 2289$ and $\overline{P}\tau_b/C = 13.3$ K determined previously for the dry system and adjust only the value ω_0 of the cut-off frequency. From the experimental value of ω_0, provided that the thermal inertia of the bridges remains negligible compared to that of the beads, we can easily determine the thermal resistance of the contact R which is found to decrease when the bridge diameter ϕ is increased (Fig. 13).

The theoretical description of the thermal resistance associated with a bead-bead contact of finite size decorated by a liquid bridge is, to our knowledge, not yet available. The extension of the model, briefly summarized in Section 3.1.3, to this latter case appears to be difficult and we will limit the discussion of the experimental results to a few comments.

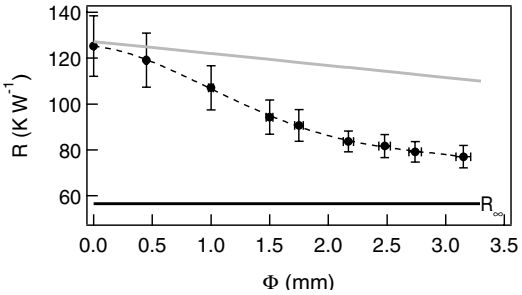

Fig. 13. Resistance R vs. bridge diameter Φ. We observe that the thermal resistance of the contacts decreases when the diameter of the liquid bridge is increased. The dashed line is a guide for the eye while the horizontal black line corresponds to the value, $R_\infty = 56.6$ K W^{-1}, estimated for beads totally immersed in oil [from equations (7) and (8) with $A = 1.7$]. The grey line corresponds to equation (9).

First, we can obtain an estimate of the thermal resistance R_∞, one would measure for beads immersed in silicon oil, and compare this latter value to the minimum of R reported in Figure 13. The thermal conductivity of the silicon oil k_{so} is 0.16 W m^{-1} K^{-1}. In this case, $\zeta \simeq 101$ and $\xi \simeq 2.4$ (for $F = 100$ N). Replacing k_a by k_{so} in equation (8), we get $\mathcal{H}_0(\zeta) \simeq 5.33 + A$, which accounts for the heat transport through the fluid layer around the contact (A is again a constant of the order of unity). Moreover, we know from reference [2] that, for a value of ξ as small as 2.4, the value $2\xi/\pi \simeq 1.5$ largely overestimates the real value of $\mathcal{H}_c(\xi)$, which is associated with the conduction through the contact circle of radius ρ, and that the correction $\Delta\mathcal{H}_m(\xi)$ remains much smaller than unity. Thus, we can neglect $\mathcal{H}_c(\xi)$ and $\Delta\mathcal{H}_m(\xi)$ in equation (7), which leads to $R_\infty \simeq 398/(5.33 + A)$ K W^{-1}. If we assume that the value $A = 1.7$ remains unchanged when the beads are immersed in air or in silicon oil, we get $R_\infty \simeq 56.6$ K W^{-1} (Fig. 13). We observe that the resistance of the contact R approaches R_∞ when the diameter Φ of the liquid bridge is increased. Even if R remains about 30% larger than R_∞ for $\Phi/d \simeq 0.3$, we consider that the agreement between our experimental data and the theoretical estimate of R_∞ again reinforce the validity of our measurements. Moreover, the model tells us that, in the case of beads immersed in oil, the heat is mainly transfered through the liquid layer around the contact region and not through the circle of contact (indeed, $\mathcal{H}_c(\xi) \ll \mathcal{H}_0(\zeta)$). We expect the conclusion to hold true in the case of a large liquid bridge decorating the contact region. This provides us with an important clue for understanding the smooth variation of R with the diameter ϕ of the bridge.

We could expect, from equations (7) and (8) and from the ratio air- to oil-conductivity, R to suddenly decrease when the liquid is introduced in the contact region. However, we observe experimentally that R decreases almost linearly as Φ is increased. This feature may be qualitatively understood as follows: in the case of dry beads, about half of the heat is transfered through the real bead-bead contact, the second half passing through the air gap around the contact in spite of the small radius ρ of the contact circle. Think now about what would happen, if the radius ρ was slightly increased by $\delta\rho$. We would mainly expect $\mathcal{H}_c(\xi)$ to increase linearly with $\delta\rho$ as $\mathcal{H}_c(\xi) \propto \rho$, $\Delta\mathcal{H}_m(\xi)$ to remain negligible, and $\mathcal{H}_0(\zeta)$ not to change. Note that to increase ρ by $\delta\rho$ is equivalent to decorating the contact with a steel bridge of diameter $\Phi = 2(\rho + \delta\rho)$. The corresponding variation δR of the resistance would then be given by $\delta R = -R\delta\rho/\rho$ {from equation (7), $\delta[\log_e(R)] = -\delta[\log_e(\mathcal{H}_c)]$}. Thus, the introduction in the contact region of a small quantity of oil, whose conductivity is smaller than that of steel, is expected only to decrease continuously the resistance of the contact and not to produce any discontinuous change in R. If we assume that the addition of oil produces the same effect as the addition of steel except that the transport of heat occurs in oil instead of in steel, we can roughly estimate

$$\frac{\delta R}{R} = -\frac{k_{so}}{k_s}\frac{\Phi - 2\rho}{2\rho} \tag{9}$$

which leads to $\frac{dR}{d\Phi} \simeq -5.2$ K W^{-1} mm^{-1}. As the presence of the liquid bridge also modifies the temperature field in the bead, leading to a spreading of the temperature-field lines and, thus, to reduced thermal resistance. The slope given by equation (9) is expected to overestimate the experimental value for small Φ, which is observed experimentally (Fig. 13). Obviously, due to assumptions which remain open to criticism, this quantitave estimate must be considered with caution. However, we consider that the reasoning presented above is qualitatively correct for explaining the smooth dependency of the resistance R on the diameter Φ, when the contact region is decorated by a liquid bridge.

4 Conclusions

First, we would like to point out several flaws in our experimental situation; due to long thermal times (especially $2\pi/\omega_0 \simeq 15$ mn) the experimental times are long [for instance, more than 10 hours are needed to measure $H^{(n)}(\nu)$ at five relevant frequencies ν]; the study of R as a function of the applied force F or of the nature of the surrounding gas, which is in principle possible, would require a huge experimental effort. Indeed, at least the times τ_b and τ_c would depend on F or on the nature of the surrounding gas, so a characterization of the whole experimental setup would be necessary. The analysis could not be limited to the response of the system at a given position n in the chain, which would increase significantly the experimental time. Note, however, that the behavior of $H^{(n)}(\nu)$ as a function of n at one given frequency ν would be, in principle, enough for determining ω_0. Such studies remain to be done although we already attempted, before drawing our conclusions, to measure the resistance of the contacts in air, nitrogen, carbon dioxide and helium and obtained sensible qualitative-results. However, these studies were limited to the thermal response at a given position n as a function of the frequency ν, which unfortunately turned out not to be sufficient to determine R afterwards.

In conclusion, we have shown that the study of the heat transport along a chain of beads is a pertinent way to access the thermal properties of the contact. The experimental method is applied successfully to the case of dry contacts in the sense that the measured resistance R can be accounted for by a classical model by Batchelor et al. [2]. We made use of the experimental setup for studying the effect of liquid bridges decorating the contact regions and observed a smooth decrease in the thermal resistance when the diameter of the bridge is increased. Even if a theoretical description of this latter experimental situation is not yet available, simple arguments, which extend the dry-contact model, allow us to understand, at least qualitatively, the experimental results. This work provides important clues for understanding the transport of heat in partially wet granular materials.

The authors would like to thank C. Tassius and E. Freyssingeas for careful reading and useful criticism of the manuscript.

Appendix: Modeling of the experimental situation

We observe experimentally that the temperature oscillation at a given frequency ν decreases exponentially when n increases and tends to a finite value for large values of n. These experimental observations are accounted for by the following modeling of the experimental system (Fig. 10).

The thermal conductivity of the chain can be accounted for as follows: we consider each bead as a thermal mass, C, in contact with its two neighbors (except bead 1) through identical thermal resistors, R. We assume that the thermal losses through the PTFE plates, which are used to align the beads, can be described as the effect of a single thermal resistor, β, which connects locally each bead to the remaining part of the experimental setup. Let us denote $T^{(n)}(t)$ the temperature of the bead n at time t. We can thus write, taking $\omega_0 \equiv 2/(RC)$ and $\tau_c \equiv \beta C$,

$$\frac{\partial T^{(n)}}{\partial t} = \frac{\omega_0}{2}\left[T^{(n+1)} + T^{(n-1)} - 2T^{(n)}\right] - \frac{1}{\tau_c}\left[T^{(n)} - T_f(x_n)\right] \quad (n>1) \qquad (10)$$

where $T_f(x_n)$ denotes the temperature of the experimental setup at the position $x_n \equiv (n-1)d$ of the bead n (diameter d). We will assume that the chain is long enough to be considered as semi-infinite: the boundary condition far away from the heat source is then written as $T^{(n+1)} = T^{(n)}$, $(n \to \infty)$. We will further assume that the contact between the first bead with the metallic part, that constrains the chain along its axis, can be described by a simple thermal resistor, γ. The first bead is heated by injecting the heating power $P(t)$ so that the energy balance leads to (taking $\tau_b \equiv \gamma C$)

$$\frac{\partial T^{(1)}}{\partial t} = \frac{\omega_0}{2}\left[T^{(2)} - T^{(1)}\right] - \frac{1}{\tau_b}\left[T^{(1)} - T_f(0)\right] + \frac{P}{C}. \qquad (11)$$

Let us now assume that the experimental setup, apart from the PTFE plates and the chain, behaves like a semi-infinite rod (diffusion coefficient D) in contact with the outside atmosphere (at temperature T_a) through the conductance per unit length $1/\eta$. Furthermore, we assume that the thermal contact between the beads and the rod along the chain is bad enough for the temperature of the rod not to be affected by the corresponding heat sources (i.e. β is large and the diffusion in the rod is fast). As a consequence, we can write:

$$\frac{\partial T_f}{\partial t} = D\Delta T_f - \frac{1}{\tau_l}(T_f - T_a). \qquad (12)$$

where $\tau_l = \eta C_f$ is the characteristic time associated with the thermal losses to the atmosphere (here C_f is the heat capacity per unit length of the metallic frame). We will consider that the temperature profile $T_f(x,t)$ only results from energy injection at $x=0$ from bead 1 (we thus assume that $\gamma \ll \beta$). Writing the energy balance at the contact between bead 1 and the rod leads to:

$$\frac{T^{(1)} - T_f(0)}{\gamma} = -DS\nabla T_f(0) \qquad (13)$$

where S stands for the cross section of the rod.

After having written the general set of equations (10) and (12) and the boundary conditions (11) and (13), we consider the harmonic response of the experimental setup as a function of the frequency $\nu = \omega/(2\pi)$ by writing:

$$T_f(x,t) = T_0 \exp(j\omega t - k_f x), \qquad (14)$$

$$T^{(n)}(t) = T_0^{(n)} \exp(j\omega t), \qquad (15)$$

and

$$P(t) = \overline{P}(\omega)\exp(j\omega t). \qquad (16)$$

From equation (12), we get $k_f^2 = \frac{\eta + j\omega}{D}$ whereas the boundary condition (13) leads to $T_0^{(1)} = T_0(1+\alpha)$ with $\alpha \equiv \gamma DSk_f$. In addition, equation (10) imposes:

$$T_0^{(n)} = T_0^{(0)}\exp[-(n-1)k] + T_0\frac{\exp[-(n-1)k_f d]}{1 + \omega_0\tau_c[1-\cosh(k_f d)] + j\omega\tau_c} \qquad (17)$$

with $\cosh(k) = \left[1 + \frac{1}{\omega_0\tau_c}\right] + j\frac{\omega}{\omega_0}$. The constants $T_0^{(0)}$ and T_0 are obtained as functions of $\overline{P}$ by using the second boundary condition (11).

In the limit $|k_f d| \ll 1$, which is well satisfied in our experimental conditions, equation (17) reduces to

$$\frac{CT_0^{(n)}}{\overline{P}\tau_b} = \Big\{1 + [\alpha + j(1+\alpha)\omega\tau_c]\exp[-(n-1)k]\Big\}/ \Big\{(1+j\omega\tau_c)[\alpha + j(1+\alpha)\omega\tau_b] + \frac{1}{2}\omega_0\tau_b[1-\exp(-k)][\alpha + j(1+\alpha)\omega\tau_c]\Big\}. \quad (18)$$

We point out that the diffusion coefficient in the rod, D, only appears, in this final expression proposed for $|T_0^{(n)}|$, in the coefficient α. We are in the limit $|nk_f d| \ll 1$, which leads to $|k_f d| \ll 1$ when we consider the limit $n \gg 1$ (the diffusion in the rod is fast) but, even in this limit, $\alpha \equiv \gamma DSk_f$ can remain finite. Note that, from equation (18), the amplitude $T_0^{(n)}$ of the temperature oscillations decreases exponentially when n is increased and reaches, for n large, the value, $T_0^{(\infty)}$ which magnitude remains finite as observed experimentally [Fig. 9, Eq. (4)].

References

1. E. Branly, C. R. Acad. Sc. Paris **111**, 785 (1890)
2. G.K. Batchelor, F.R.S., R.W. O'Brien, Proc. R. Soc. London, Ser. A **355**, 313 (1997)
3. E. Falcon, B. Castaing, M. Creyssels, Eur. Phys. J. B **38**, 475 (2004), and references therein
4. C.-H. Liu, S. R. Nagel, Phys. Rev. B **48**, 15646 (1993)
5. C. Coste, B. Gilles, Eur. Phys. J. B **7**, 155 (1999)
6. See the websites of some glasswool producers, for instance: Isover (`http://www.isover.com/`) Isofam (`http://www.isofam.net/`)
7. I. Engelhardt, S. Finsterle, C. Hofster, Vadose Zone J. **2**, 239 (2003)
8. G. Kling, Forsh. Geb. Ingenieurwes. **9**, 28 (1938)
9. H.J. Leyers, Chem.-Ing.-Tech. **44**, 1109 (1972)
10. G.J. Cheng, A.B. Yu, P. Zulli, Chemical Engineering Science **54**, 4199 (1999)
11. J.-C. Geminard, H. Gayvallet, Phys. Rev. E **64**, 041301 (2001)
12. L. Landau, E. Lifchitz, *Theory of elasticity* (Pergamon Press, NY, 1959)